Int J Adv Manuf Technol (2016) 83:2143–2157
DOI 10.1007/s00170-015-8112-0

ORIGINAL ARTICLE

An offline predictive feedrate scheduling method for parametric interpolation considering the constraints in trajectory and drive systems

Lei Lu[1] · **Lei Zhang**[1] · **Shijun Ji**[1] · **Yanjun Han**[1] · **Ji Zhao**[1]

Received: 19 June 2015 / Accepted: 12 November 2015 / Published online: 23 November 2015

Abstract The ability of drive unit limits the velocity, acceleration, and jerk of the axis, and the process and tool path geometry constrain the feedrate, acceleration, and jerk of the trajectory. It is of great difficulty and importance to schedule a suitable feedrate profile to achieve the higher machining efficiency and satisfy all the constraints. Due to the complexity of the feedrate scheduling algorithm, this paper presents an offline predictive feedrate scheduling method considering the constraints of trajectory system and drive system. The constraints in the drive system are transformed to the trajectory system appropriately, which reduces the difficulty of feedrate scheduling. The one-dimensional high-order time-optimal problem is solved by a numerical calculation method according to the bang-bang control method. The predictive method is applied to find the switching points of the jerk. Then a time-optimal feedrate profile under all the constraints is obtained. Both simulations and experiments are carried out to prove the effectiveness of the proposed offline predictive feedrate scheduling method.

Keywords Feedrate scheduling · Transformation of constraints · Predictive deceleration · Parametric interpolation

1 Introduction

Many scholars devote to increase the machining precision and efficiency. Some of them improve the smoothness of the tool path in order to amplify the real feedrate and to reduce the machining time [1–3]. Other scholars enhance the precision and efficiency of the machine tool by improving dynamic characteristics [4–6] and optimizing the feedrate profiles [7–27]. For machining process, the feedrate in trajectory system is a very important process parameter. The value and changing rate of feedrate affect the machining efficiency and quality. And for a given machine tool, the drive dynamic characteristics impose restrictions on the feedrate, acceleration, and jerk of the individual axis. Therefore, it is a meaningful and tough thing to schedule an efficient feedrate profile under various constraints.

In the early literatures, the constraints mostly considered are limited to the feedrate and the acceleration in the trajectory system. Bobrow et al. [7] and Shin and McKay [8] switch the acceleration ($\ddot{s}$) between its maximum and minimum limits at the identified path points to generate a bang-bang style trajectory. Dong and Stori [9] draw the velocity limit curve in the $\dot{s}-\ddot{s}$ phase plane and use bidirectional scan algorithm for constrained feedrate optimization in $\dot{s}-\ddot{s}$ phase plane. Other mathematical optimization methods, such as dynamic programming (DP) [10] or Pontryagin's minimum principle [11], are also applied to solve the optimal feedrate problem more efficiently. Afterwards, the jounce or jerk in the trajectory system is also considered. Lai et al. [12] and Fan et al. [13] determine the feasible maximal feedrate at the critical points and use the jounce or jerk confined acceleration/deceleration profile to connect the feedrate profile in the trajectory system.

Although some literatures consider the constraints in the drive system, only the worst-case axis is generally considered. Dong et al. [14] extend the bidirectional method by using bidirectional scan minimum-time feedrate optimization algorithm to find the optimal feedrate profile. Zhang et al. [15, 16] give a discrete and computationally efficient algorithm to find

✉ Lei Zhang
prozhanglei@126.com

[1] School of Mechanical Science and Engineering, Jilin University, Changchun 130025, People's Republic of China

a sequence of globally optimal velocity points under the feedrate, acceleration, and chord error bounds.

With increasing requirements for machining accuracy, the jerk as a constraint has to be considered for it is related to the frequency of the input trajectory. In order to make full use of the machine dynamic performance, the considered constraints are no longer confined in the trajectory system. The constraints in the drive system need to be considered. It not only increases the number of constraints but also makes the problem more complicated, resulting in difficulty to find the optimal solution. Altintas and Erkorkmaz [17] define the displacement profile as a quintic spline of time along the tool path and optimize the travel time of each segment through nonlinear optimization method. Afterwards, Sencer and Altintas [18] use B-spline curve to represent the feedrate profile and convert the feedrate optimization problem to a nonlinear optimization through simplifying the constraints and it is solved by using sequential quadratic method. Zhang [19] and Fan [20] transform the feedrate scheduling problem to a convex optimization problem, and then it is solved by optimization method. Erkorkmaz and Heng [21] propose an intelligent heuristic rules in optimal process and computational load is reduced compared with gradient-based optimal methods. Ridwan et al. [22] adjust the feedrate automatically by using fuzzy adaptive control method. In addition to the optimization algorithm, segment feedrate planning [23, 24] is also a common method, in which the critical points are found according to the constraints and the curve is split at the critical points. The feedrate profile is scheduled in each segment and then combined. The segment feedrate planning method has higher computational efficiency but it is too conservative. There are some other methods such as look-ahead method and iteration method. Beudaert et al. [25] iteratively compute the intersection of the displacements at each time step according to the constraints and choose the maximum displacement to obtain the optimal feedrate profile. Sun et al. [26, 27] create the analytical relations between feedrate and the arc length parameter, and through proportional iterative adjustment, the target feedrate profile is obtained without violating constraints. Although the solution obtained by the iterative method is more optimal than the segment feedrate planning method, the robust and computation efficiency of those methods are limited.

For the complexity of the feedrate scheduling, this paper attempts to propose an offline predictive feedrate scheduling method. The feedrate scheduling method considers the velocity, acceleration, and jerk constraints not only in the trajectory system but also in the drive system. Firstly, the constraints are classified into the constraints in the trajectory system and drive system. The constraints in the drive system are transformed to the trajectory system properly in this paper. Then the multidimensional high-order time-optimal problem becomes the one-dimensional high-order time-optimal problem. It can be solved by numerical calculation method according to the bang-bang control principle [28]. At last, the proposed offline predictive feedrate scheduling method is validated through both simulations and experimental tests on two complex non-uniform rational basis spline (NURBS) curves.

2 Parametric interpolation

Figure 1 illustrates the whole process of parametric interpolation. The tool path is planned according to the requirements of processing and the tool path generated by CAM is discrete points. The discrete points need to be fitted to parameter curve for it is not convenient for parametric interpolator. The feedrate profile is planned according to the tool path curve, processing requirements, and the dynamic characteristics of the machine tool. The parametric interpolator uses the tool path curve and the feedrate profile to calculate the next interpolation point in every interpolation period. And the kinematical transformation is used to produce the control signals that command the servo axis movements respecting the constraints of trajectory and drive systems.

According to the parametric interpolation algorithm, the next interpolation point u_{i+1} is calculated by the current interpolation point u_i and the feedrate. In order to yield the desired arc length accurately, the second-order series interpolator is chosen as

$$u_{i+1} = u_i + \frac{du_i}{dt}T + \frac{1}{2}\left(\frac{d^2u_i}{dt^2}\right)T^2 + \text{H.O.T.} \quad 0 \le u \le 1 \tag{1}$$

where T is the sampling period and H.O.T. represents the high-order truncation error and u is the tool path parameter. And

$$\frac{du}{dt} = \sigma^{-1}\dot{s} \tag{2}$$

$$\frac{d^2u}{dt^2} = -\sigma^{-3}\sigma'\dot{s}^2 + \sigma^{-1}\ddot{s} \tag{3}$$

where s is the arc length of the tool path, $\dot{s}$ *and* $\ddot{s}$ are the feedrate and acceleration in the trajectory system, and σ and σ' are the first and second derivatives of the path arc length with respect to the curve parameter.

3 Feedrate optimization problem

3.1 Constraints in the trajectory system

As shown in Fig. 2, taking no account of the specific kinematical structure, the cutting tool is running along a certain path. The feedrate, acceleration, and jerk of the cutting tool along the path constitute the trajectory system.

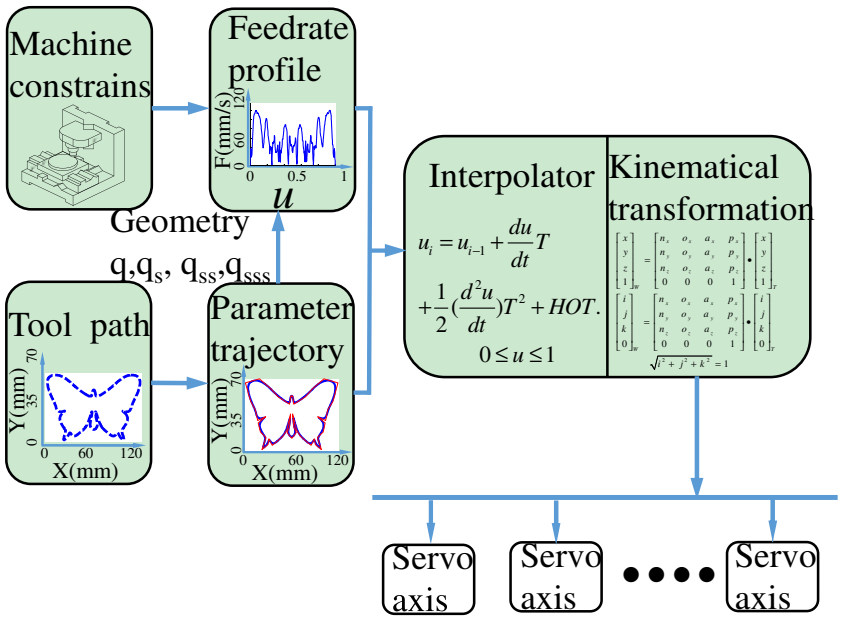

Fig. 1 Parametric curve interpolation process

Generally, the maximum feedrate, acceleration, and jerk in the trajectory system are given according to the machining process. For different machining processes, different constraints for the feedrate, acceleration, and jerk in the trajectory system are given. For example, in the literature [29], the relationship between feedrate and cutting force in the milling process is found and the specified resultant cutting force constrains the feedrate in the trajectory system. In numerical control, the output of interpolator is the sampled axis setpoints. In order to ensure the geometric accuracy, the chord error needs to be limited. According to the interpolation principle, the chord error is expressed by

$$\delta(u) = \rho(u) - \sqrt{\rho^2(u) - \left(\frac{\dot{s}\,(u)T}{2}\right)^2} \tag{4}$$

where T is the interpolator period and ρ is the radius of curvature at the parameter position u of the path curve. For a given chord error limit $\delta_{\max}$, the feedrate is constrained by

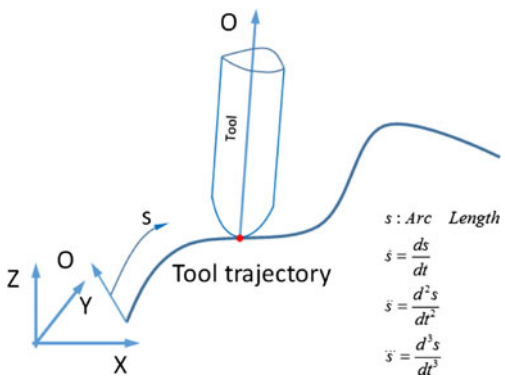

Fig. 2 The trajectory system

$$\dot{s}\,(u) \le {}^{2\sqrt{\rho^2(u) - (\rho(u) - \delta_{\max})^2}}/_{T} \tag{5}$$

Obviously, in the trajectory system, the kinematical parameters are related to the machining process closely. Almost all the constraints in machining process can be transformed into the constraints of the feedrate, acceleration, and jerk in the trajectory system. The forms of the constraints are given as

$$\dot{s} \le F_{\lim}, \left|\ddot{s}\right| \le A_{\lim}, \left|\dddot{s}\right| \le J_{\lim} \tag{6}$$

where $\dot{s}$, $\ddot{s}$, and $\dddot{s}$ are the feedrate, acceleration, and jerk in the trajectory system, and $F_{\lim}$, $A_{\lim}$, and $J_{\lim}$ are the limited feedrate, acceleration, and jerk in the trajectory system. $F_{\lim}$, $A_{\lim}$, and $J_{\lim}$ considered in this paper only refer to the prescribed maximum of feedrate, acceleration, and jerk.

3.2 Constraints in the drive system

The contour accuracy of the tool path is determined by the tracking error in each axis of machine tool. The tracking error is related to the velocity, acceleration, and jerk of the motion axis. Therefore, the constraints of the tracking error and the vibration limit the velocity, acceleration, and jerk of the motion axis [30]. For a specific drive, the acceleration is also limited by the torque and linear region of the motor, and too larger jerk can excite the vibration.

The constraints in the drive system are summarized by

$$\left\{|\dot{q}|, \left|\ddot{q}\right|, \left|\dddot{q}\right|\right\}_i \le \left\{\dot{q}, \ddot{q}, \dddot{q}\right\}_{i\max} \tag{7}$$

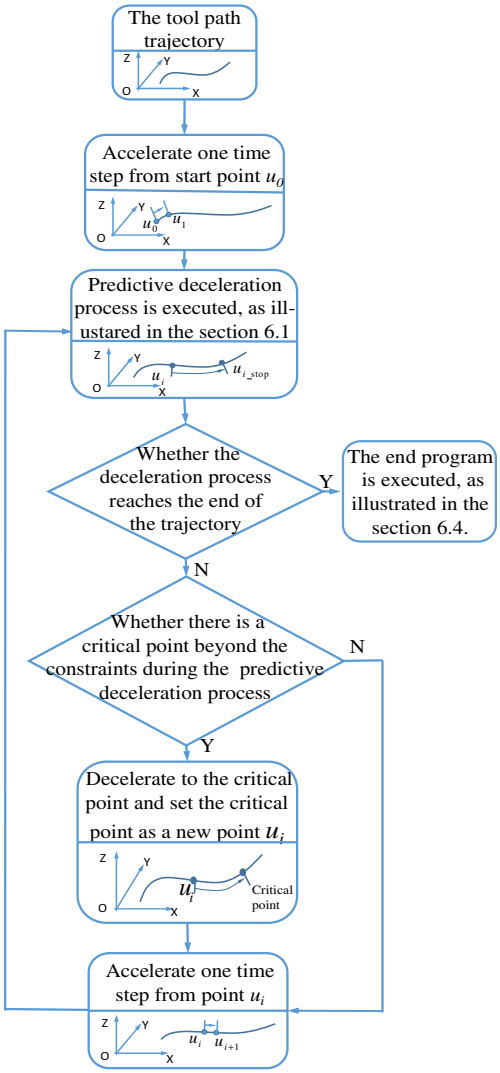

Fig. 3 The feedrate scheduling method in the trajectory system

where $\{|\dot{q}|, |\ddot{q}|, |\dddot{q}|\}_i$ represents the velocity, acceleration, and jerk of the i-axis, and $\{\dot{q}, \ddot{q}, \dddot{q}\}_{i\max}$ represents the prescribed maximum velocity, acceleration, and jerk of the i-axis.

Using the formula for the derivative of the composition of two functions, it is possible to express the velocity of the drive $\dot{q}$ as a function of the trajectory geometry q_s multiplied by a function of the feedrate in the trajectory system $\dot{s}$, i.e.,

$$\dot{q} = \frac{dq}{dt} = \frac{dq}{ds}\frac{ds}{dt} = q_s\,\dot{s} \tag{8}$$

And from Eq. (8), $\ddot{q}$ and $\dddot{q}$ can be derived as

$$\ddot{q} = q_{ss}\dot{s}^2 + q_s\ddot{s} \tag{9}$$

$$\dddot{q} = q_{sss}\dot{s}^3 + 3q_{ss}\,\dot{s}\,\ddot{s} + q_s\dddot{s} \tag{10}$$

where q_s, q_{ss}, *and* q_{sss} are the first, second, and third derivatives of the axis positions with respect to the path displacement. Therefore, the kinematic parameters of the drives are related to the geometry of the trajectory and the kinematical parameters in the trajectory system.

3.3 Time-optimal feedrate problem

For a multi-axis system and a target trajectory, the problem of identifying an optimal feedrate profile under all the constraints is a nontrivial optimal process problem, i.e.,

$$\begin{aligned} &\min\left(T_{\Sigma}\right) = \min\left(\int_0^1 \dot{s}\,(u)^{-1}\sigma du\right) \quad \text{subject to} \\ &\dot{s} \le F_{\lim}, \quad |\ddot{s}| \le A_{\lim}, \quad |\dddot{s}| \le J_{\lim} \\ &\left\{|\dot{q}|, |\ddot{q}|, |\dddot{q}|\right\}_i \le \left\{\dot{q}, \ddot{q}, \dddot{q}\right\}_{i\max} \end{aligned} \tag{11}$$

It is a computational cost issue to solve the problem using a general mathematical method. Convergence in these algorithms is sensitive to the initial condition and calculating steps. If the inappropriate calculating steps and convergence threshold are chosen, it is prone to diverge and impossible to find the solution.

4 Transformation of the constraints

The trajectory system is a one-dimensional system, and the dimension of the drive system is determined by the number of the motion axis. In this paper, the feedrate profile is scheduled in the trajectory system. The nonlinear and coupling relations between the constraints in the trajectory system and those in the drive system given by Eqs. (8)–(10) are considered. Therefore, the constraints in the drive system need to be transformed to the trajectory system appropriately.

According to Eqs. (7) and (8), the velocity constraints in the drive system can be expressed by

$$\left|q_s^i\,\dot{s}\right| \le \dot{q}_{i\max} \tag{12}$$

where q_s^i is the first derivative of the axis positions with respect to the path displacement for the i-axis. Because of $\dot{s} \ge 0$ in the trajectory system, Eq. (12) can be changed as

$$\dot{s} \le {\dot{q}_{i\max}}/{|q_s^i|} \tag{13}$$

According to Eq. (7), applying the triangle inequality $|A+B| \le |A|+|B|$ to Eq. (9) yields the expression for the constraints of acceleration as

$$\left|\ddot{q}_i\right| = \left|q_{ss}^i\dot{s}^2 + q_s^i\ddot{s}\right| \le \left|q_{ss}^i\dot{s}^2\right| + \left|q_s^i\ddot{s}\right| \le \ddot{q}_{i\max} \tag{14}$$

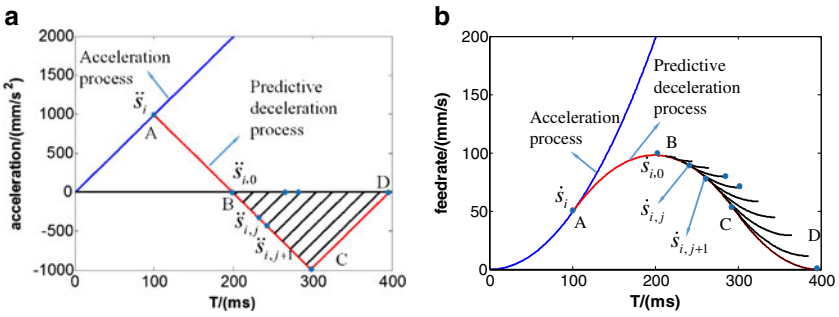

Fig. 4 The deceleration process. **a** The acceleration profile. **b** The feedrate profile

There is still a coupling term of the $\dot{s}$ and $\ddot{s}$ in Eq. (14). So scaling factors δ_1 and δ_2 are introduced to decouple Eq. (14), i.e.,

$$\begin{cases} \left|q^i_{ss}\dot{s}^2\right| \le \delta_1 \ddot{q}_{i\max} \\ \left|q^i_s \ddot{s}\right| \le \delta_2 \ddot{q}_{i\max} \end{cases} \tag{15}$$

δ_1 and δ_2 are constant, and they are selected according to the machine tool and trajectory characteristics.

According to Eqs. (7) and (10), the jerk constraints in the drive system can be expressed by

$$\left|\dddot{q}_i\right| \le \left|q^i_{sss}\dot{s}^3 + 3q^i_{ss}\,\dot{s}\,\ddot{s} + q^i_s\dddot{s}\right| \le \left|q^i_{sss}\dot{s}^3\right| + \left|3q^i_{ss}\,\dot{s}\,\ddot{s}\right| + \left|q^i_s\dddot{s}\right| \le \dddot{q}_{i\max} \tag{16}$$

By the similar approach applied to acceleration constraints, the jerk constraint is transformed to

$$\begin{cases} \left|q^i_{sss}\dot{s}^3\right| \le \mu_1 \dddot{q}_{i\max} \\ \left|3q^i_{ss}\,\dot{s}\,\ddot{s}\right| \le \mu_2 \dddot{q}_{i\max} \\ \left|q^i_s\dddot{s}\right| \le \mu_3 \dddot{q}_{i\max} \end{cases} \tag{17}$$

where μ_1, μ_2, and μ_3 are constant scaling factors, and they are also selected according to the machine tool and trajectory characteristics.

According to the Eqs. (13), (15), and (17), the transformations between the constraints in the drive system and those in the trajectory system are listed as

$$\dot{s} \le \dot{q}_{i\max}\Big/_{\left|q^i_s\right|} \begin{cases} \dot{s} \le \sqrt{\delta_1 \ddot{q}_{i\max}\Big/\left|q^i_{ss}\right|} \\ \left|\ddot{s}\right| \le \delta_2 \ddot{q}_{i\max}\Big/\left|q^i_s\right| \end{cases} \begin{cases} \dot{s} \le \sqrt[3]{\mu_1 \dddot{q}_{i\max}\Big/\left|q^i_{sss}\right|} \\ \left|\dot{s}\,\ddot{s}\right| \le \mu_2 \dddot{q}_{i\max}/3\left|q^i_{ss}\right| \\ \left|\dddot{s}\right| \le \mu_3 \dddot{q}_{i\max}\Big/\left|q^i_s\right| \end{cases} \tag{18}$$

Now the coupled multi-dimensional constrained optimization problem is transformed to constrained optimization problem in the trajectory system, i.e., Eq. (11) is changed as

$$\min\left(T_{\sum}\right) = \min\left(\int_0^1 \dot{s}^{-1}(u)\sigma du\right) \quad \text{subject to}$$

$$\begin{cases} \dot{s} \le F_{\lim} \\ \dot{s} \le \dot{q}_{i\max}\Big/\left|q^i_s\right| \\ \dot{s} \le \sqrt{\delta_1 \ddot{q}_{i\max}\Big/\left|q^i_{ss}\right|} \\ \dot{s} \le \sqrt[3]{\mu_1 \dddot{q}_{i\max}\Big/\left|q^i_{sss}\right|} \end{cases}, \begin{cases} \ddot{s} \le A_{\lim} \\ \left|\ddot{s}\right| \le \delta_2 \ddot{q}_{i\max}\Big/\left|q^i_s\right| \\ \left|\dot{s}\,\ddot{s}\right| \le \mu_2 \dddot{q}_{i\max}\Big/3\left|q^i_{ss}\right| \end{cases}, \begin{cases} \dddot{s} \le J_{\lim} \\ \left|\dddot{s}\right| \le \mu_3 \dddot{q}_{i\max}\Big/\left|q^i_s\right| \end{cases} \tag{19}$$

Scheduling the feedrate only in the trajectory system greatly reduces the difficulty of the optimal problem.

5 Discretization and numerical calculation

The feedrate, acceleration, and jerk are calculated using discretized numerical integration method, and the constant time step T is chosen according to the curvature of the trajectory. The kinematical parameters for i+1-th point in the trajectory can be calculated by the kinematical parameters for ith point, i.e.,

$$\begin{aligned} \ddot{s}_{i+1} &= \ddot{s}_i + \dddot{s}_{i+1}T \\ \dot{s}_{i+1} &= \dot{s}_i + \ddot{s}_i T + \dddot{s}_{i+1}T^2\Big/2 \\ s_{i+1} &= s_i + \dot{s}_i T + \ddot{s}_i T^2\Big/2 + \dddot{s}_{i+1}T^3\Big/6 \end{aligned} \tag{20}$$

where $\dddot{s}_{i+1}$ is calculated by jerk constraints in the ith point.

The curve parameter of the i+1-th point is calculated by using Taylor expansion as

$$u_{i+1} \approx u_i + u^i{}_s \Delta s + u^i{}_{ss}\Delta s^2/2 + u^i{}_{sss}\Delta s^3/6 \tag{21}$$

where $u_s{}^i$, $u_{ss}{}^i$, and $u_{sss}{}^i$ are the first, second, and third derivatives of the curve parameter with respect to the path displacement for the i-axis. Δs is the displacement from the ith point to the i+1-th point and is expressed by

$$\Delta s_{i+1} = s_{i+1} - s_i \tag{22}$$

According to Eqs. (8)–(10), the velocity, acceleration, and jerk of the i+1-th point in the drive system are calculated by

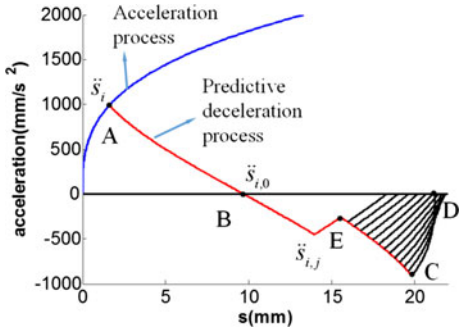

Fig. 5 The deceleration process

$$\begin{aligned}\dot{q}_{i+1} &= q_s^{i+1}\,\dot{s}_{i+1}\\ \ddot{q}_{i+1} &= q_{ss}^{i+1}\,\dot{s}_{i+1}^2 + q_s^{i+1}\,\ddot{s}_{i+1}\\ \dddot{q}_{i+1} &= q_{sss}^{i+1}\dot{s}_{i+1}^3 + 3q_{ss}^{i+1}\dot{s}_{i+1}\ddot{s}_{i+1} + q_s^{i+1}\dddot{s}_{i+1}\end{aligned} \tag{23}$$

6 Feedrate scheduling method in the trajectory system

After the time optimal problem with multi-dimensional constraints is transformed to one-dimensional problem, i.e., Eq. (19), it can be solved by numerical calculation method according to the bang-bang control principle. The time-optimal profile is a bang-bang style trajectory generated by the jerk switching between its maximum and minimum limits. The whole process of the feedrate scheduling method is shown in Fig. 3. In the accelerating process, the maximum jerk is chosen, and in the decelerating process, the minimum jerk is chosen. There are three main modules in the feedrate scheduling method: (1) the predictive deceleration process, (2) the acceleration forward process, and (3) the end program. The predictive deceleration process is the key module of the feedrate scheduling method. The main function of the predictive deceleration process is to find the critical points where the constraints are violated and determine the switching points of the jerk.

6.1 Predictive deceleration process

For the constraints of the jerk and acceleration, the acceleration and feedrate cannot change abruptly. However, in a practical process, the tool path is arbitrary and it makes the constraints changing abruptly. Therefore, the trajectory needs to accelerate or decelerate in advance to guarantee the feedrate, acceleration, and jerk not beyond the constraints. In order to ensure the optimality of the deceleration process, the decelerating process needs to be planned. The acceleration and feedrate profiles of predictive decelerating process are shown in Fig. 4. As shown in Fig. 4, the *A–B* segment indicates the process in which the acceleration decreases to zero, the *B–C* segment indicates the acceleration-decreasing process and the black lines indicate the acceleration-increasing process. The predictive decelerating process from one trajectory point $\{u_i, \dot{s}_i, \ddot{s}_i, \dddot{s}_i\}$ illustrated in Fig. 4 is described by the following steps in details.

Step 1: Determine whether the acceleration in the trajectory point $\{u_i, \dot{s}_i, \ddot{s}_i, \dddot{s}_i\}$ is greater than zero. If not, set the trajectory point $\{u_i, \dot{s}_i, \ddot{s}_i, \dddot{s}_i\}$ as $\{u_{i,0}, \dot{s}_{i,0}, \ddot{s}_{i,0}, \dddot{s}_{i,0}\}$, then go to step 3.

Step 2: As shown by the segment *A–B* in Fig. 4, decelerate forward under the minimum jerk until the acceleration is zero and obtain the new trajectory point $\{u_{i,0}, \dot{s}_{i,0}, \ddot{s}_{i,0}, \dddot{s}_{i,0}\}$.

Step 3: As shown in Fig. 4, decelerate one time step under the minimum jerk from the trajectory point $\{u_{i,j}, \dot{s}_{i,j}, \ddot{s}_{i,j}, \dddot{s}_{i,j}\}$ and obtain the new trajectory point $\{u_{i,j+1}, \dot{s}_{i,j+1}, \ddot{s}_{i,j+1}, \dddot{s}_{i,j+1}\}$.

Step 4: As shown by the black line indicating the increasing process of acceleration in Fig. 4, decelerate forward under the maximum jerk from the trajectory point $\{u_{i,j+1}, \dot{s}_{i,j+1}, \ddot{s}_{i,j+1}, \dddot{s}_{i,j+1}\}$ until the acceleration increases to zero.

Step 5: Let $j=j+1$.

Step 6: Determine whether the feedrate is zero when the acceleration is zero. If not, then go to step 3.

Step 7: Exit the predictive deceleration process.

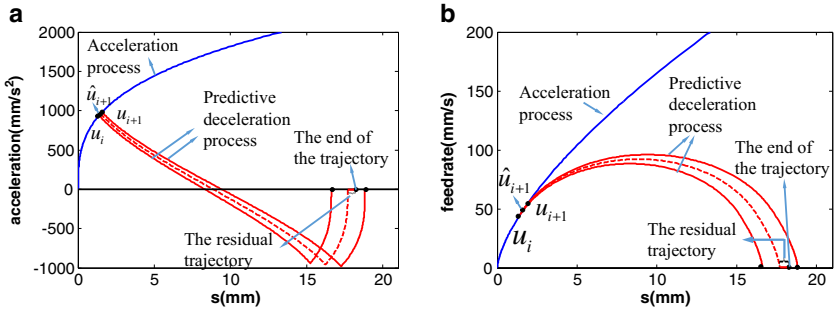

Fig. 6 The deceleration process. **a** The acceleration profile. **b** The feedrate profile

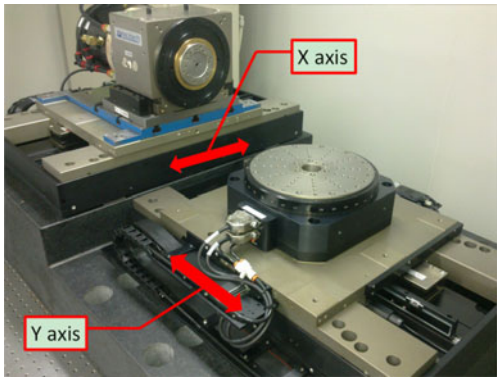

Fig. 7 The experiment platform

6.2 Checking the constraints in the predictive deceleration process

During the predictive deceleration process as illustrated in Section 6.1, the constraints need to be checked at the same time. According to the numerical calculation method, the jerk is calculated by the constraints. Therefore, the constraints of the feedrate and acceleration need to be checked further. In order to ensure the optimality of the efficiency, it cannot decelerate immediately when there is a point violating the constraints during the predictive deceleration process. When there are points violating the feedrate and acceleration constraints in different phases, the corresponding measures need to be taken.

6.2.1 Case A: checking the constraints during the process of the acceleration decreasing to zero

During the process of the acceleration decreasing to zero as indicated by the *A–B* segment in Fig. 4, if there is a point violating the feedrate or acceleration constraints, the violating point is a critical point. The trajectory needs to decelerate to the critical point by the minimum jerk from the point u_i according to the predictive deceleration process.

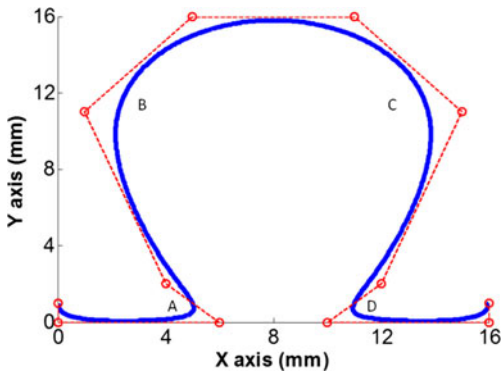

Fig. 8 The curve of case one

Table 1 The constraints of the machine tool drives

	X	*Y*
V_{max} (mm/s)	100	100
A_{max} (mm/s^2)	900	900
J_{max} (mm/s^3)	15,000	15,000

6.2.2 Case B: checking the constraints during the acceleration decreasing process

During the acceleration-decreasing process as indicated by the *B–C* segment in Fig. 4, if there is a point violating the acceleration constraints, the jerk at this point is recalculated by the acceleration constraints and the other kinematical parameters are recalculated according to Eqs. (20)–(23). Then the predictive deceleration process continues.

During the acceleration decreasing process as indicated by the *B–C* segment in Fig. 4, if there is a point violating the feedrate constraints, this point is a critical point and the trajectory needs to decelerate to the critical point from the point u_i according to the predictive deceleration process.

6.2.3 Case C: checking the constraints during the acceleration increasing process

During the acceleration-increasing process from the point $\{u_{i,j}, \dot{s}_{i,j}, \ddot{s}_{i,j}, \dddot{s}_{i,j}\}$ as indicated by the black line in Fig. 4, if there is a point violating the acceleration constraints, this acceleration-increasing process needs to be stopped. As shown in Fig. 5, *E* represents the point that violates the acceleration constraints. The predictive deceleration process continues from the point *E* until the feedrate and acceleration are reduced to zero.

During the acceleration-increasing process from the point $\{u_{i,j}, \dot{s}_{i,j}, \ddot{s}_{i,j}, \dddot{s}_{i,j}\}$ as indicated by black line in Fig. 4, if there is a point violating the feedrate constraints, this acceleration-increasing process is stopped and the new point $\{u_{i,j+1}, \dot{s}_{i,j+1}, \ddot{s}_{i,j+1}, \dddot{s}_{i,j+1}\}$ is obtained by decelerating one-time step. Then another acceleration-increasing process starts from the point $\{u_{i,j+1}, \dot{s}_{i,j+1}, \ddot{s}_{i,j+1}, \dddot{s}_{i,j+1}\}$. If the feedrate still violates the constraints in this point, the above process is repeated until the feedrate satisfies the constraints in this point. And the point where the feedrate satisfies the constraints is a critical point and the trajectory decelerates to the critical point from point u_i.

Table 2 The constraints in the trajectory system

$\dot{s}_{max}$ (mm/s)	$\ddot{s}_{max}$ (mm/s^2)	$\dddot{s}_{max}$ (mm/s^3)
150	1000	10,000

Table 3 The transform factors of the constraints

	δ_1	δ_2	μ_1	μ_2	μ_3
Value	0.5	0.7	0.4	0.4	0.7

6.3 Acceleration forward process

If there is no critical point violating the constraints in the predictive deceleration process from point u_i, according to Eqs. (20)–(23), an acceleration forward process is executed that the new trajectory point u_{i+1} is obtained by accelerating one-time step with the maximum jerk. The constraints of the acceleration and feedrate are not considered in the acceleration forward process and those need to be further checked.

During the acceleration forward process, if the acceleration or the feedrate violates the constraints, the jerk is recalculated by Eq. (24) or Eq. (25), respectively, according to the corresponding constraints, i.e.,

$$\dddot{s}_{i+1} = \left(\ddot{s}_{\lim} - \ddot{s}_i\right) \Big/ T \tag{24}$$

$$\dddot{s}_{i+1} = 2\left(\dot{s}_{\lim} - \dot{s}_i - \ddot{s}_i T\right) \Big/ T^2 \tag{25}$$

where $\ddot{s}_{\lim}$ and $\dot{s}_{\lim}$ are the acceleration constraint and the feedrate constraint, respectively. The other kinematical parameters are recalculated by Eqs. (20)–(23).

6.4 The end program

In every predictive deceleration process, whether the end of the trajectory is reached has to be checked. However, due to the existence of discretization error, it is impossible to reach the end of the trajectory exactly when both the feedrate and acceleration are reduced to zero. The appropriate point near the end of the trajectory when both the feedrate and acceleration are zero is searched by using the dichotomy method.

As shown in Fig. 6, if the end of the trajectory is overtaken in the predictive deceleration process from the trajectory point u_{i+1}, the new trajectory point $\hat{u}_{i+1}$ is recalculated by halving the time intervals T. The deceleration process from the new trajectory point $\hat{u}_{i+1}$ is represented by the red dotted line as shown in the Fig. 6. If the deceleration process still overtakes the end of the trajectory, the time interval T needs to be further halved. If the deceleration process is not beyond the end of the trajectory and the residual trajectory satisfies the error requirements, the trajectory decelerates according to the deceleration process.

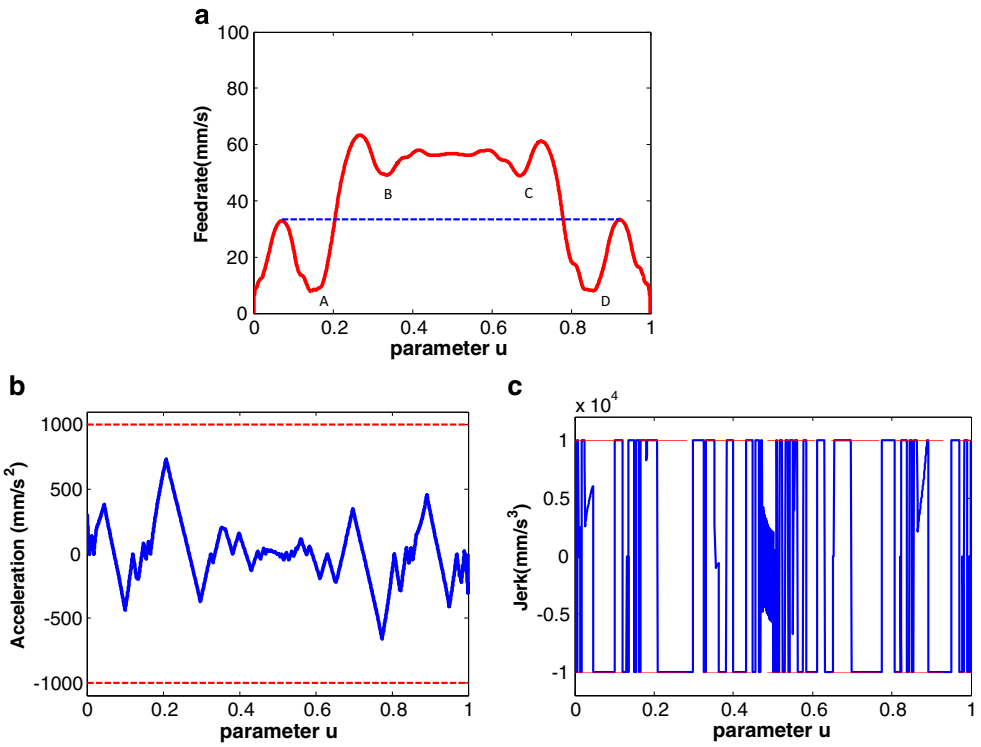

Fig. 9 The case one results after scheduling. **a** The feedrate profile. **b** The acceleration profile. **c** The jerk profile

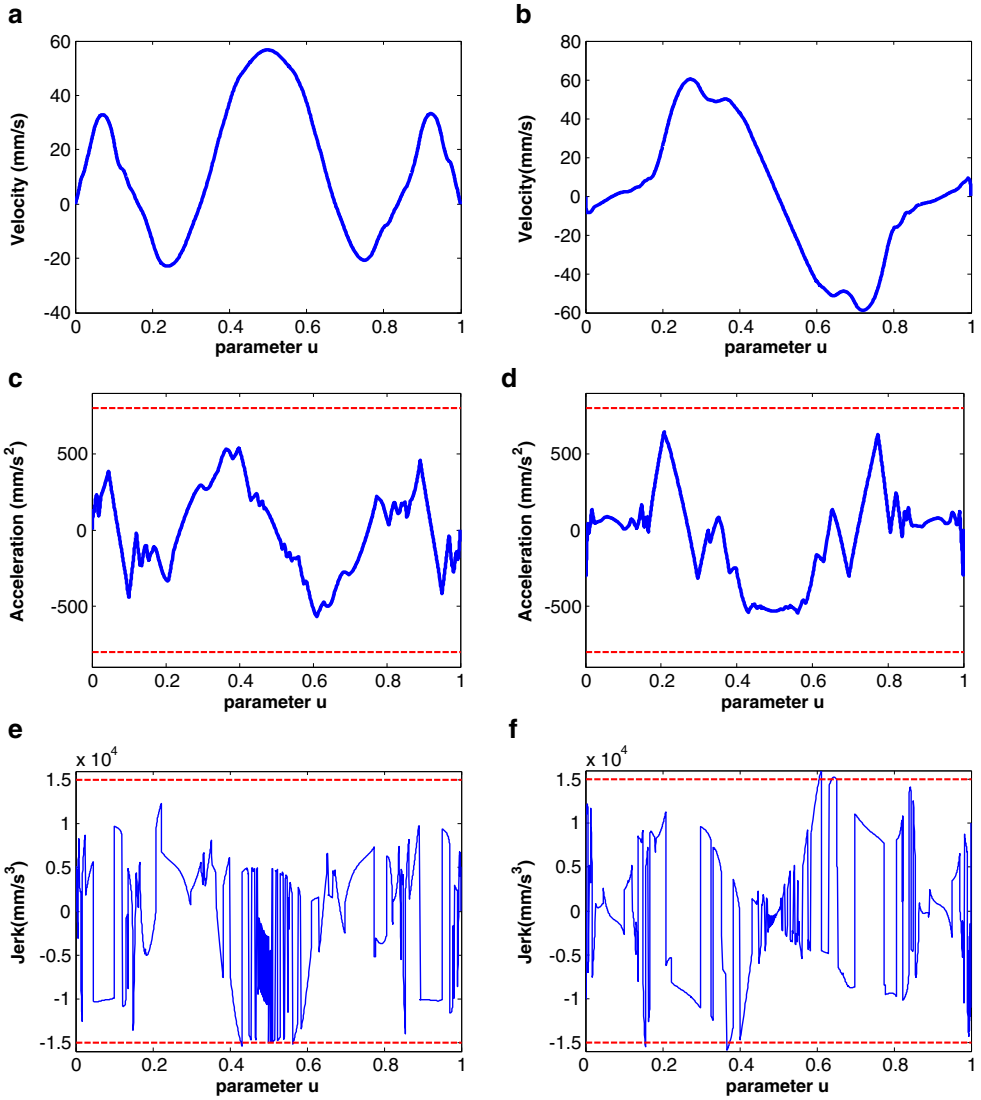

Fig. 10 The case one results of simulation. **a** The *X*-axis velocity. **b** The *Y*-axis velocity. **c** The *X*-axis acceleration. **d** The *Y*-axis acceleration. **e** The *X*-axis jerk. **f** The *Y*-axis jerk

7 Fitting the feedrate profile

When the feedrate profile is scheduled, a series of discrete feedrate data points $\dot{s}_i$ are obtained. It is not convenient for parametric interpolation to use the discrete data points. Therefore, it is necessary to fit the discrete data points for parametric interpolation. Different from the regular curve fitting, the fitting of discrete feedrate data points to generate a feedrate profile not only requires the feedrate to satisfy the error requirement but also the acceleration and jerk calculated by the feedrate profile to satisfy the error requirements. The least squares fitting of the B-spline [31] is applied to the fitting of feedrate profile, which will be discussed in the further paper in details.

8 Simulations and experiments

The feasibility and applicability of feedrate scheduling method proposed in this paper are verified by simulations and experiments for two complex NURBS curves. The feedrate profile considering the constraints both in the trajectory and drive systems is scheduled using the feedrate scheduling method. In the simulation, a parametric interpolator using the Eq. (1) is programmed by MATLAB software. The trajectory points for each motion axis in every interpolation cycle are generated by the parametric interpolator according to the specific trajectory and the feedrate profile. The velocity, acceleration, and jerk for each motion axis can be obtained

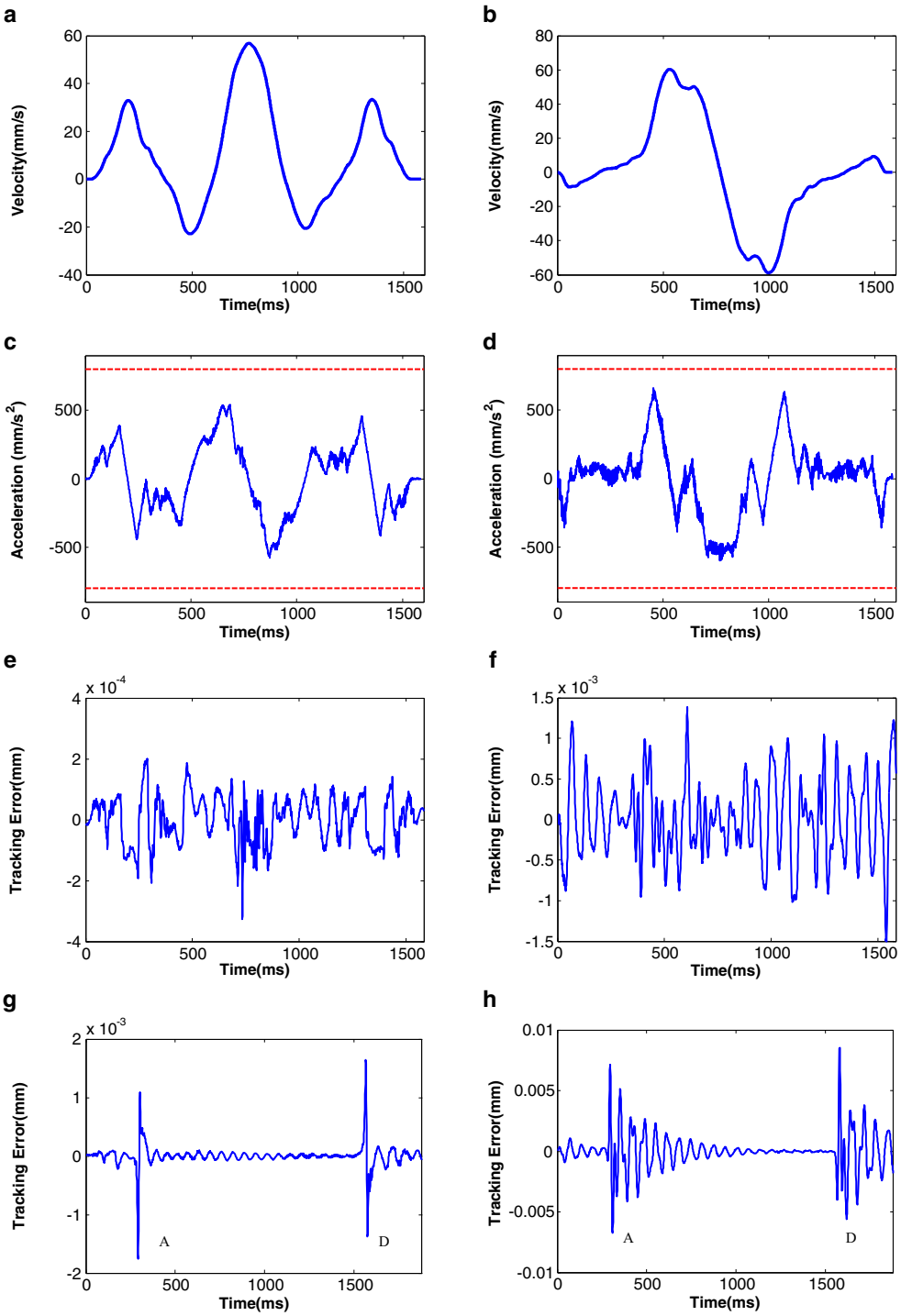

Fig. 11 The case one results of the experiment. **a** The *X*-axis velocity. **b** The *Y*-axis velocity. **c** The *X*-axis acceleration. **d** The *Y*-axis acceleration. **e** The *X*-axis tracking error. **f** The *Y*-axis tracking error. **g** The *X*-axis tracking error of constant feedrate. **h** The *Y*-axis tracking error of constant feedrate

according to the trajectory points generated by the parametric interpolator. Whether they satisfy the constraints of velocity, acceleration, and jerk for each motion axis is checked by the simulation.

The experiments are carried out on a two-drive platform as shown in Fig. 7, which is controlled by the PC-based open motion controller. The platform is driven by linear motor and the resolution of the linear encoder is ±0.5 μm. A special interpolator is designed on the open motion controller for our own purpose, and the interpolator period is chosen as 1 ms. The controller is able to read the position every 0.125 ms in real time and can provide the velocity and acceleration of each axis.

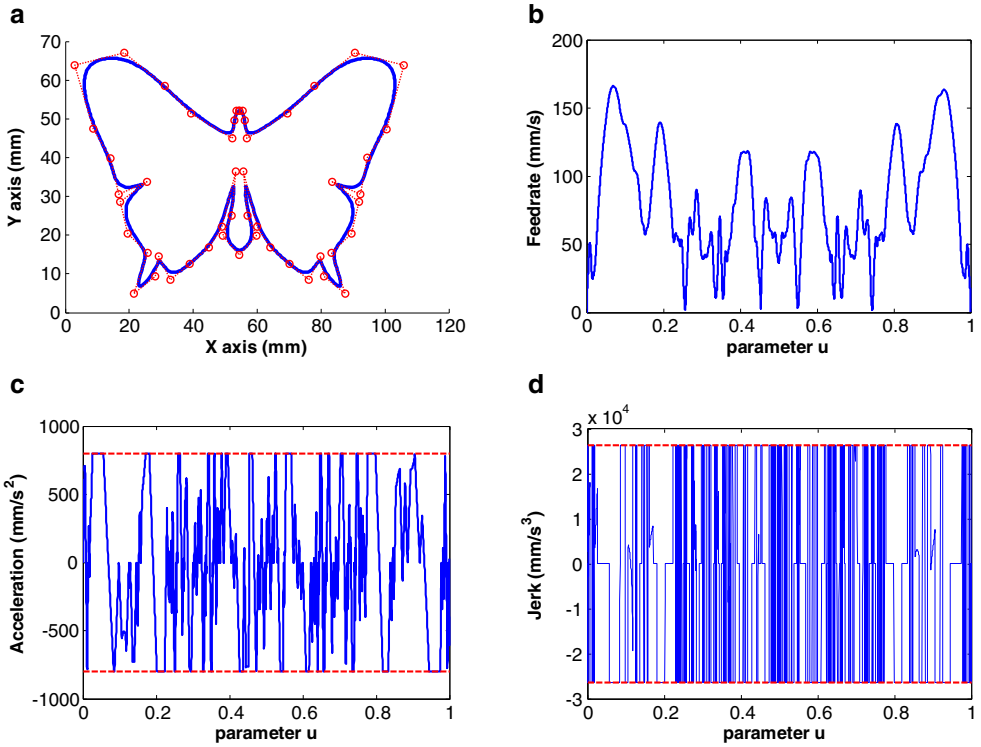

Fig. 12 The results of case two. **a** The curve of case two. **b** The feedrate profile. **c** The acceleration profile. **d** The jerk profile

8.1 Case one

Figure 8 illustrates the NURBS curve for case one. The parameters of the curve are listed as follows:

$$\begin{aligned} P &= \left\{ \begin{bmatrix} 0 \\ 1 \end{bmatrix}, \begin{bmatrix} 0 \\ 0 \end{bmatrix}, \begin{bmatrix} 6 \\ 0 \end{bmatrix}, \begin{bmatrix} 4 \\ 2 \end{bmatrix}, \begin{bmatrix} 1 \\ 11 \end{bmatrix}, \begin{bmatrix} 5 \\ 16 \end{bmatrix}, \begin{bmatrix} 11 \\ 16 \end{bmatrix}, \begin{bmatrix} 15 \\ 11 \end{bmatrix}, \begin{bmatrix} 12 \\ 2 \end{bmatrix}, \begin{bmatrix} 10 \\ 0 \end{bmatrix}, \begin{bmatrix} 16 \\ 0 \end{bmatrix}, \begin{bmatrix} 16 \\ 1 \end{bmatrix} \right\} \\ \omega &= \{1.0, 2.0, 2.0, 1.0, 1.0, 1.0, 1.0, 1.0, 1.0, 2.0, 2.0, 1.0\} \\ U &= \left\{ 0, 0, 0, 0, 0.111, 0.2222, 0.3333, 0.4444, 0.5556, 0.6667, 0.8889, 1, 1, 1, 1 \right\} \\ K &= 3 \end{aligned} \tag{26}$$

where P, ω, U, and K are the control points, weight, knot vectors, and degree.

The curve for case one is symmetrical, and it has four curvature critical points obviously as indicated by A, B, C, and D in Fig. 8. According to the constraints, the feedrate profile is related to those critical points in Cartesian coordinate system. Therefore, the feedrate profile is also symmetrical and has four corresponding critical points.

The feedrate scheduling method is executed by MATLAB. In this case, the computation time on a PC (the PC with 3.1-GHz CPU and 4-G memory) is about 2 min when the time interval T is 1 ms. The computation time can be further improved if a larger time interval T is chosen and the data structure and calculation algorithm are further optimized. As shown in Table 1, the kinematic constraints in the drive system are listed, and the kinematic constraints in the trajectory in this case are listed in the Table 2. According to feedrate scheduling method proposed in this paper, the range of the scale factors for the constraints transformation is

$$\begin{cases} 1 \le \delta_1 + \delta_2 \le 1.5 \\ 1 \le \mu_1 + \mu_2 + \mu_3 \le 1.5 \end{cases} \tag{27}$$

They are selected according to the platform's kinematical characteristics and the curvature of the curve. The selected scale factors are listed in Table 3.

The feedrate profile scheduled by the method are illustrated in the Fig. 9. As shown in Fig. 9a, the feedrate satisfies the constraints in the trajectory system. Corresponding to the symmetry and the curvature critical points of the trajectory, the feedrate profile is also symmetry and the feedrate is decreased in those critical points (points A, B, C, D). According to Eqs. (9) and (10), the acceleration and jerk of the axis are related with the feedrate in the trajectory system and the geometrical characteristic. Due to the curvature of those points, the feedrate in the trajectory system is decreased for the axis' acceleration and jerk constraints. As shown in Fig. 9b, the acceleration in the trajectory is also under the constraints. As

Table 4 The constraints of the machine tool drives

	X	Y
V_{max} (mm/s)	220	220
A_{max} (mm/s^2)	800	800
J_{max} (mm/s^3)	26,400	26,400

Table 5 The constraints in the trajectory system

$\dot{s}_{max}$ (mm/s)	$\ddot{s}_{max}$ (mm/s^2)	$\dddot{s}_{max}$ (mm/s^3)
220	800	26,400

the length of the curves and critical points, the maximum acceleration is not reached and the acceleration increases in the slope way as shown in Fig. 9b. The jerk is also under the constraints as shown in Fig. 9c. As shown in Fig. 9c, the jerk is switched in the maximum and minimum jerk constraints to

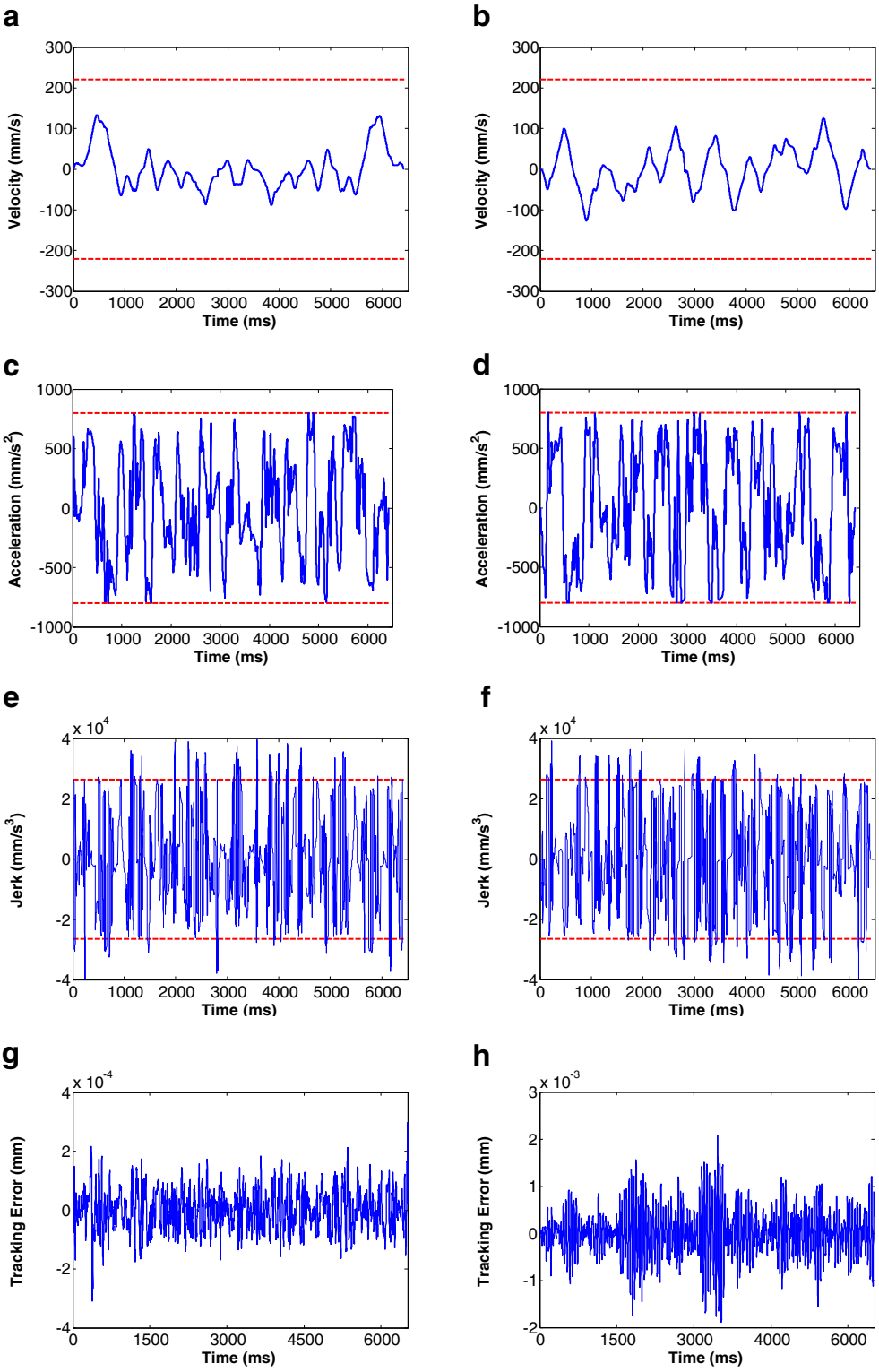

Fig. 13 The results of case two. **a** The *X*-axis velocity. **b** The *Y*-axis velocity. **c** The *X*-axis acceleration. **d** The *Y*-axis acceleration. **e** The *X*-axis jerk. **f** The *Y*-axis jerk. **g** The *X*-axis tracking error. **h** The *Y*-axis tracking error

generate a bang-bang style trajectory according to the minimum principle. It is demonstrated that the trajectory accelerates and decelerates in the maximum acceleration and deceleration ability.

In order to verify that the constraints in the drive system are satisfied, the simulation is carried out. The interpolation equation used in the simulation is Eq. (1) and the interpolation period is 1 ms. The velocity, acceleration, and jerk for each motion axis are calculated by the differential operation of the trajectory points generated by the interpolator in the simulation. The simulated velocity and acceleration for *X*-axis and *Y*-axis are given in Fig. 10, which shows that the kinematical parameters for each drive are under the constraints. As shown in Fig. 10e, f, the jerk for *X*-axis and *Y*-axis is under the constraints mostly. Although the jerk is beyond the constraints in some points, it is within the 120 % authorized jerk overrun limit and it is caused by the sum of the transforming factors larger than 1 in Eq. (27).

The experiment is carried out in the platform shown in Fig. 7 to verify the validity of the feedrate profile. The tool path trajectory shown in Fig. 6 and the scheduled feedrate are input to the controller. The interpolation equation and interpolation period in the experiments are the same as those in the simulation. The position of the moving element is obtained by the linear encoders, and the velocity and acceleration are also obtained by the controller. The velocity, acceleration, and tracking error for *X*-axis and *Y*-axis in the experiments are shown in Fig. 11. In Fig. 11, the velocity and acceleration are relatively consistent with those in the simulation and satisfy the constraints. In order to compare with the scheduled feedrate profile, a relatively conservative feedrate of $\dot{s}=33mm/s$ is tested and it is represented as blue dotted line in Fig. 9a. The tracking errors of $\dot{s}=33mm/s$ for *X*-axis and *Y*-axis are shown in Fig. 11g and h, respectively. As shown in Fig. 11g, h, the tracking errors are amplified at the saturation regions along the trajectory, which leads to the violation of drive limits. However, when the feedrate is scheduled, the velocity, acceleration, and jerk of the *X*- and *Y*-axes are all under the constraints. When the platform carries out along the trajectory with the scheduled feedrate profile, the tracking errors of the *X*- and *Y*-axes are uniform in the whole trajectory as shown in Fig. 11e and f, respecively. The availability of the feedrate scheduled method proposed in this paper is demonstrated.

8.2 Case two

A more complex butterfly curve as shown in Fig. 12a is also selected to verify the feasibility and applicability of feedrate scheduling method proposed in this paper. The chosen transforming factors are listed in Table 3. In order to validate the optimal of the scheduled feedrate, the kinematical characteristics chosen in this case are same as the kinematical characteristics selected in [24]. The kinematical characteristics in the drive system are given in Table 4, and the kinematical characteristics in the trajectory system are given in Table 5. For information, the computation time on MATLAB is about 2.5 min.

Table 6 Cycle time comparison for scheduling results

Optimization strategy	Cycle time (s)
Predictive scheduling method	6.42
Segments feedrate planning method [24]	8.1

The scheduled results are shown in Fig. 12, and the feedrate, acceleration, and jerk in the trajectory system are all under the corresponding constraints. Although the tool path trajectory is complexity and the number of the critical points is numerous, the feedrate profile can be scheduled appropriately. It is demonstrated that the feedrate planning method can schedule the feedrate profile properly no matter how complex the tool path is or not. Corresponding to the symmetry and the curvature critical points of the trajectory, the feedrate profile is also symmetrical and the feedrate is decreased in those critical points.

The experiment is also carried out in the platform shown in Fig. 7. The velocity, acceleration, and tracking error for *X*-axis and *Y*-axis in the experiments are shown in Fig. 13. The velocity, acceleration, and jerk (it is obtained by the output of the controller) are under the constraints of the drive. The tracking errors are small and show no obvious regional characteristics although the butterfly curve is complex.

As shown in the Table 6, an overall 20 % cycle time reduction is realized for the whole tool path compared with the feedrate result scheduled by the segment feedrate planning method [24]. The optimal of the scheduled feedrate is demonstrated compared with the segment feedrate planning method. The tracking error is less than 1 μm, indicating that the cycle time reduction does not come at the expense of the drives' dynamic accuracy. The experimental results show that the machine can be operated under the constraints and the capability of each motion axis is fully used after the feedrate is scheduled.

9 Conclusions

In order to avoid the complicated and heavy calculations in real time, this paper presents an offline feedrate scheduling method. Compared with the usual offline feedrate scheduling methods, the novelty of the method proposed in this paper is that the feedrate is scheduled in the trajectory system. Moreover, the constraints in the drive system are transformed to the trajectory system properly. For all kinematic constraints to be classified into the constraints in the trajectory or drive system,

all those kinematic constraints no matter the contour error or drive's ability to limit can be considered. In addition, the difficulty of the scheduling method is reduced for the constraints in the drive system are transformed to those in the trajectory system by the transforming factors. According to the minimum principle, the feedrate scheduling problem in the trajectory system can be solved and the time optimal solution is the bang-bang style solution, i.e., the jerk switches between the maximum and minimum available value. Discrete feedrate data points are obtained by the feedrate scheduling method. After those feedrate points are fitted by B-spline, the proposed method gives a solution, which is closed to the optimal mathematical solution under all the constraints. The performances of the proposed feedrate scheduling method are validated by simulation and experimental results.

Acknowledgments The authors are grateful for the financial support from the National High Technology Research and Development Program (863 Program) of China (Grant No. 2012AA041304), the National Key Basic Research and Development Program (973 program) of China (Grant No. 2011CB706702), and the Specialized Research Fund for the Doctoral Program of Higher Education of China (Grant No. 20110061110022).

References

1. Beudaert X, Pechard P-Y, Tournier C (2011) 5-Axis tool path smoothing based on drive constraints. Int J Mach Tools Manuf 51(12):958–965. doi:10.1016/j.ijmachtools.2011.08.014
2. Zhang LB, You YP, He J, Yang XF (2010) The transition algorithm based on parametric spline curve for high-speed machining of continuous short line segments. Int J Adv Manuf Technol 52(1–4):245–254. doi:10.1007/s00170-010-2718-z
3. Ernesto CA, Farouki RT (2011) High-speed cornering by CNC machines under prescribed bounds on axis accelerations and toolpath contour error. Int J Adv Manuf Technol 58(1–4):327–338. doi:10.1007/s00170-011-3394-3
4. Altintas Y, Erkorkmaz K, Zhu WH (2000) Sliding mode controller design for high speed feed drives. CIRP Ann Manuf Technol 49(1):265–270. doi:10.1016/s0007-8506(07)62943-6
5. Pritschow G, Croon N (2013) Ball screw drives with enhanced bandwidth by modification of the axial bearing. CIRP Ann Manuf Technol 62(1):383–386. doi:10.1016/j.cirp.2013.03.086
6. Varanasi KK, Nayfeh SA (2004) The dynamics of lead-screw drives: low-order modeling and experiments. J Dyn Syst Meas Control 126(2):388–396
7. Bobrow JE, Dubowsky S, Gibson J (1985) Time-optimal control of robotic manipulators along specified paths. Int J Robot Res 4:3–17
8. Shin K, McKay N (1985) Minimum-time control of robotic manipulators with geometric path constraints. IEEE Trans Autom Control 30:531–541
9. Dong J, Stori JA (2006) A generalized time-optimal bidirectional scan algorithm for constrained feed-rate optimization. J Dyn Syst Meas Control 128(2):379. doi:10.1115/1.2194078
10. Shin KG, McKay ND (1986) A dynamic programming approach to trajectory planning of robotic manipulators. IEEE Trans Autom Control 131(6):491–500
11. Gourdeau R, Schwartz HM (1989) Optimal control of a robot manipulator using a weighted time-energy cost function. Decision and Control, 1989. Proceedings of the 28th IEEE Conference on. IEEE, 1628–1631
12. Lai J-Y, Lin K-Y, Tseng S-J, Ueng W-D (2007) On the development of a parametric interpolator with confined chord error, feedrate, acceleration and jerk. Int J Adv Manuf Technol 37(1–2):104–121. doi:10.1007/s00170-007-0954-7
13. Fan W, Gao X-S, Yan W, Yuan C-M (2012) Interpolation of parametric CNC machining path under confined jounce. Int J Adv Manuf Technol 62(5–8):719–739. doi:10.1007/s00170-011-3842-0
14. Dong J, Ferreira PM, Stori JA (2007) Feed-rate optimization with jerk constraints for generating minimum-time trajectories. Int J Mach Tools Manuf 47(12–13):1941–1955. doi:10.1016/j.ijmachtools.2007.03.006
15. Zhang K, Yuan C-M, Gao X-S (2012) Efficient algorithm for time-optimal feedrate planning and smoothing with confined chord error and acceleration. Int J Adv Manuf Technol 66(9–12):1685–1697. doi:10.1007/s00170-012-4450-3
16. Zhang K, Yuan C-M, Gao X-S, Li H (2012) A greedy algorithm for feedrate planning of CNC machines along curved tool paths with confined jerk. Robot Comput Integr Manuf 28(4):472–483. doi:10.1016/j.rcim.2012.02.006
17. Altintas Y, Erkorkmaz K (2003) Feedrate optimization for spline interpolation in high speed machine tools. CIRP Ann Manuf Technol 52(1):297–302. doi:10.1016/s0007-8506(07)60588-5
18. Sencer B, Altintas Y, Croft E (2008) Feed optimization for five-axis CNC machine tools with drive constraints. Int J Mach Tools Manuf 48(7–8):733–745. doi:10.1016/j.ijmachtools.2008.01.002
19. Zhang Q, Li S-R (2013) Efficient computation of smooth minimum time trajectory for CNC machining. Int J Adv Manuf Technol 68(1–4):683–692. doi:10.1007/s00170-013-4790-7
20. Fan W, Gao X-S, Lee C-H, Zhang K, Zhang Q (2013) Time-optimal interpolation for five-axis CNC machining along parametric tool path based on linear programming. Int J Adv Manuf Technol 69(5–8):1373–1388. doi:10.1007/s00170-013-5083-x
21. Erkorkmaz K, Heng M (2008) A heuristic feedrate optimization strategy for NURBS toolpaths. CIRP Ann Manuf Technol 57(1):407–410. doi:10.1016/j.cirp.2008.03.039
22. Ridwan F, Xu X, Ho FCL (2012) Adaptive execution of an NC program with feed rate optimization. Int J Adv Manuf Technol 63(9–12):1117–1130. doi:10.1007/s00170-012-3959-9
23. Heng M, Erkorkmaz K (2010) Design of a NURBS interpolator with minimal feed fluctuation and continuous feed modulation capability. Int J Mach Tools Manuf 50(3):281–293. doi:10.1016/j.ijmachtools.2009.11.005
24. Lee A-C, Lin M-T, Pan Y-R, Lin W-Y (2011) The feedrate scheduling of NURBS interpolator for CNC machine tools. Comput Aided Des 43(6):612–628. doi:10.1016/j.cad.2011.02.014
25. Beudaert X, Lavernhe S, Tournier C (2012) Feedrate interpolation with axis jerk constraints on 5-axis NURBS and G1 tool path. Int J Mach Tools Manuf 57:73–82. doi:10.1016/j.ijmachtools.2012.02.005
26. Sun Y, Bao Y, Kang K, Guo D (2013) An adaptive feedrate scheduling method of dual NURBS curve interpolator for precision five-axis CNC machining. Int J Adv Manuf Technol 68(9–12):1977–1987. doi:10.1007/s00170-013-4816-1
27. Sun Y, Zhao Y, Bao Y, Guo D (2014) A novel adaptive-feedrate interpolation method for NURBS tool path with drive constraints. Int J Mach Tools Manuf 77:74–81. doi:10.1016/j.ijmachtools.2013.11.002
28. Bryson AE, Ho YC (1975) Applied optimal control: optimization, estimation and control. Wiley, New York
29. Erkorkmaz K, Layegh SE, Lazoglu I, Erdim H (2013) Feedrate optimization for freeform milling considering constraints from the

feed drive system and process mechanics. CIRP Ann Manuf Technol 62(1):395–398. doi:10.1016/j.cirp.2013.03.084

30. Guo J-X, Zhang K, Zhang Q, Gao X-S (2013) Efficient time-optimal feedrate planning under dynamic constraints for a high-order CNC servo system. Comput Aided Des 45(12):1538–1546. doi:10.1016/j.cad.2013.07.002
31. Piegl L, Tiller W (1997) The NURBS book, 2nd edn. Springer, New York